Organic LETTERS

Letter

pubs.acs.org/OrgLett

Design and Syntheses of Highly Emissive Aminobenzopyrano-xanthene Dyes in the Visible and Far-Red Regions

Shinichiro Kamino,*[,†,‡] Miho Murakami,[‡] Masaru Tanioka,[‡] Yoshinao Shirasaki,[‡] Keiko Watanabe,[†,‡] Jun Horigome,[§] Yousuke Ooyama,[∥] and Shuichi Enomoto*[,†,‡]

[†]Next-generation Imaging Team, RIKEN-CLST, Kobe-shi, Hyogo 650-0047, Japan

[‡]Graduate School of Medicine, Dentistry and Pharmaceutical Sciences, Okayama University, Okayama-shi, Okayama 700-8530, Japan

[§]Hitachi High-Tech Science Co., Ltd., Hitachinaka-shi, Ibaraki 312-8504, Japan

[∥]Department of Applied Chemistry, Graduate School of Engineering, Hiroshima University, Higashi-Hiroshima 739-8527, Japan

Supporting Information

ABSTRACT: New derivatives of aminobenzopyrano-xanthene (ABPX) dyes have been designed and synthesized with high fluorescence quantum yields in the visible and far-red regions. It was kinetically demonstrated that the structurally rigid conjugation of the xanthene moiety, which is closely related to the reduction of the nonradiative deactivation process, is an effective molecular design for the drastic enhancement of fluorescence emission efficiency.

Large planar π-conjugated fluorescent organic dyes, such as xanthenes,[1] acenes,[2] boron-dipyromethenes,[3] perylenes,[1c,4] and others,[5] have received a great deal of attention because of their potential applications as fluorescent probes for life sciences, photoactive medicines, photonics, and optoelectronics. The advantages of large planar π-conjugated organic molecules over linearly bonded fluorescent molecules such as cyanine dyes tend to include a high fluorescence quantum yield (ϕ_{fl}) and a high molar extinction coefficient (ε).[6] On the other hand, the main drawbacks of large planar π-conjugated organic molecules are generally their low solubility in conventional polar or nonpolar solvents and concentration-dependent quenching (CQ) because of attractive dipole−dipole interactions and/or effective intermolecular aromatic interactions, which rule out their use in solution.[7] Therefore, large π-conjugated organic molecules possessing high solubility in various solvents and desirable optical characteristics are continually required and their development has led to the rapid proliferation of advanced fluorescence-based techniques, the biggest growth areas being biology, medicine, chemistry, and material science.

Aminobenzopyrano-xanthene (ABPX) dyes were newly developed as one of the alternative π-conjugated fluorescent organic dyes[8] because ABPX01 **1**, the first ABPX dye to be developed as shown in Figure 1, is very soluble in a wide array of solvents and emits far-red fluorescence in a wide concentration range (<ca. 10^{-3} M), whereas conventional rhodamine dyes cannot practically emit fluorescence emission due to the CQ effect.[9] The exceptional properties of ABPX dyes should make them good candidates for optical microscopy, biological imaging, and sensing.[10] However, the fluorescence quantum yield of alkyl-substituted **1** is significantly low in various solvents. To achieve good performance in modern bioimaging techniques and solution-processable device applications, a high fluorescence quantum yield and high solubility in various media are desired. Therefore, the development of new ABPX derivatives with high fluorescence emission efficiencies is the task at hand. Herein, we report the design, syntheses, and fluorescence properties of new ABPX dyes having a rigid structural conformation to increase ϕ_{fl}.

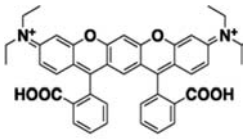

1

Figure 1. Chemical structure of aminobenzopyrano-xanthene (ABPX) dye. $ABPX01H_2^{2+}$ **1**. The *cis*- and *trans*-stereoisomers of the dicationic form are described for ABPX01 (**1a** and **1b**), respectively.

We speculated that a possible rationale for the reduction of ϕ_{fl} of **1** is that energy is lost from the excited state via thermal pathways involving the rotation of the aromatic substituents. The intramolecular mobilities of fluorophores, such as molecular vibration and rotation, are intimately related to the kinetic balance between fluorescence emission and nonradiative deactivation processes. It is a well-established design concept that the rigid conjugation of the π-conjugated skeleton by the incorporation of ring-fused structure enhances ϕ_{fl} of molecules.[7,11] Therefore, the restriction of the intramolecular mobility (RIM) of the xanthene moiety of **1** is a design

Received: November 12, 2013
Published: December 10, 2013

   dx.doi.org/10.1021/ol403262x | *Org. Lett.* 2014, 16, 258−261

Scheme 1. Syntheses of ABPX Dyes

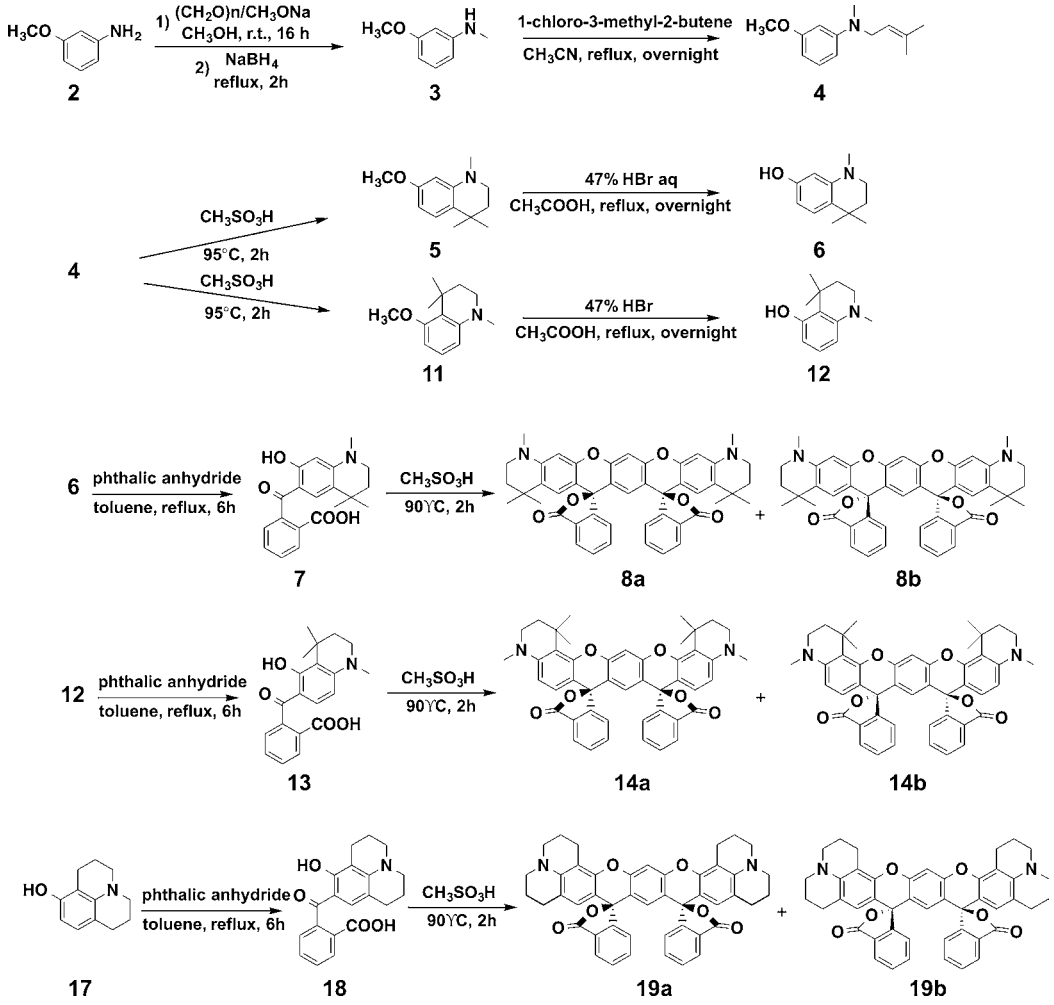

strategy. As RIM creates efficient nonradiative deactivation pathways for the decay of the excited states, modification of the xanthene moiety such that these intramolecular mobilities are restricted could increase the fluorescence emission intensity. Then, we focused on the structurally rigid conjugations around the diethylamino chains of **1**. Single bonds connected to the diethylamino group of ABPX01 freely rotate in solution. Hence, restriction of the free rotation of the diethylamino chains would lead to further enhancement of the fluorescence emission intensity. Based on these hypotheses, we designed and synthesized new ABPX derivatives in which the amino groups are incorporated into rigid six-membered rings. Then, the structure–fluorescence emission relationships are discussed.

The synthetic routes of ABPX101–103 are outlined in Scheme 1. Alkylation of 3-methoxy-*N*-methylaniline **2** using 1-chloro-3-methyl-2-butene in the presence of K_2CO_3 gave 3-methoxy-(3-methyl-2-butenyl)aniline **4** in 54% yield. Cyclization of compound **4** using neat $MeSO_3H$ at 95 °C gave regioselective quinoline derivatives **5** in 38% yield and **11** in 15% yield. Demethylation of **5** and **11** using aqueous HBr in CH_3COOH gave **6** and **12**, respectively. New benzophenone derivative 8-(2-carboxymethylbenzoyl)-7-hydroxy-1,1-dimethyl-*N*-methylquinoline **7** or 8-(2-carboxybenzoyl)-9-hydroxy-1,1-dimethyl-*N*-methylquinoline **13** was then synthesized by the acylation of **6** or **12** with phthalic anhydride. 9-(2-Carboxybenzoyl)-8-hydroxyjulolidine **18** was similarly synthesized by the acylation of 8-hydroxjulolidine **17** with phthalic anhydride according to the literature.[12] ABPX101, ABPX102, and ABPX103 were prepared by reacting the corresponding benzophenone derivatives with resorcinol in CH_3SO_3H, followed by simple purification by silica gel normal phase chromatography *via* conversion into the spirolactone form. The *cis*- and *trans*-stereoisomers of the spirolactone form were obtained for ABPX101 (**8a** and **8b**), 102 (**14a** and **14b**), and 103 (**19a** and **19b**), respectively.

To identify the relationships among chemical species, color, and fluorescence emission in solution, the absorption spectra and the fluorescence emission spectra of 5 μM ABPX dyes were measured in THF and $CHCl_3$ with various volume fractions of trifluoroacetic acid (TFA), as shown in Figures S1 and S2. The absorption spectra of the nonfluorescent spirolactone forms of **8**, **14**, and **19** showed peaks in the ultraviolet region. Chemical species transformation and spectral red shifts derived from the stepwise protonation of the xanthene moiety were observed in the visible region as the volume fraction of TFA was increased. The absorption bands of the nonfluorescent monocationic forms of ABPX101H$^+$ **9**, ABPX102H$^+$ **15**, and ABPX103H$^+$ **20** appeared in the visible wavelength region. The absorption bands of the dicationic forms of ABPX101H$_2^{2+}$ **10**, ABPX102H$_2^{2+}$ **16**, and ABPX103H$_2^{2+}$ **21** as shown in Figure 2 appeared in the long wavelength region. In all solvents, the absorption spectra of **10**, **16**, and **21** commonly exhibited

dx.doi.org/10.1021/ol403262x | *Org. Lett.* 2014, 16, 258–261

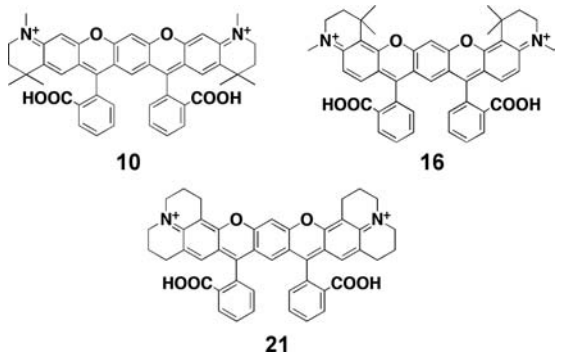

Figure 2. Chemical structures of dicationic forms of ABPX dyes. The *cis*- and *trans*-stereoisomers of the dicationic form are described for ABPX101 (**10a** and **10b**), 102 (**16a** and **16b**), and 103 (**21a** and **21b**), respectively.

vibronic bands. The longest-wavelength band was attributed to the 0−0 transition, and the second-longest band, to the 0−1 transition. The profiles of the absorption spectra and fluorescence emission spectra were almost symmetric to each other. Based on the spectral studies, we concluded that the fluorescent dicationic form is appropriate for investigations of the optical properties in solution. The protolytic equilibria of these ABPX dyes are summarized in Scheme S1. The profiles of the absorption spectra and fluorescence emission spectra of 5 μM *cis*-ABPX dyes of **10a**, **16a**, **21a**, and rhodamineB (RB) in $CHCl_3$ containing 2.5% TFA are shown in Figure 3, and a solution of them exhibits a vivid absorption color and bright fluorescence emission.

10a, **16a**, and **21a** were well dissolved and exhibited strong fluorescence in $CHCl_3$ containing 2.5% TFA. Subsequently, the optical properties of 1 μM ABPX derivatives were closely investigated in $CHCl_3$ containing 2.5% TFA. The relative fluorescence quantum yields of these derivatives were measured

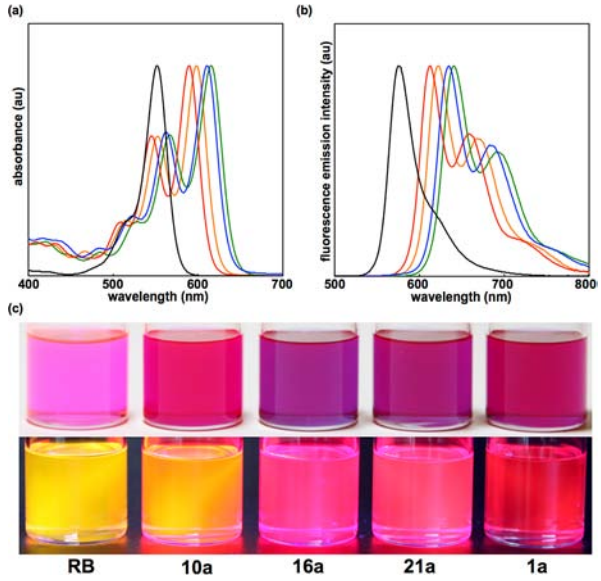

Figure 3. (a) Absorption and (b) fluorescence emission spectra of *cis*-ABPX dyes and RB in chloroform containing 2.5% TFA (black, RB; red, ABPX101 **10a**; orange, ABPX01 **1a**; blue, ABPX103 **21a**; green, ABPX102 **16a**). I_{ex} = 365 nm. (c) Absorption (upper row) and fluorescence emission (bottom row) colors of RB and *cis*-ABPX dyes in chloroform containing 2.5% TFA.

by excitation at 366 nm using reference RB dye in ethanol (ϕ_{fl} = 0.73). The relative fluorescence quantum yields of **10** (**10a**, ϕ_{fl} = 0.70; **10b**, ϕ_{fl} = 0.69), **16** (**16a**, ϕ_{fl} = 0.50; **16b**, ϕ_{fl} = 0.49), and **21** (**21a**, ϕ_{fl} = 0.55; **21b**, ϕ_{fl} = 0.54) were drastically increased relative to that of **1** (**1a**, ϕ_{fl} = 0.17; **1b**, ϕ_{fl} = 0.16). The excellent ϕ_{fl} of **10** was observed in the solvents examined and was comparable to that of highly fluorescence emitting RB (ϕ_{fl} = 0.71). All ABPX derivatives commonly exhibited well-developed bimodal fluorescence emission spectra over a wide wavelength region that included the visible and far-red regions and a significant spectral red shift relative to the spectrum of RB. The fluorescence emission spectra of **16a** (λ_{fl0-0} = 640 nm, λ_{fl0-1} = 693 nm) and **21a** (λ_{fl0-0} = 635 nm, λ_{fl0-1} = 683 nm) were red-shifted relative to that of **1** (λ_{fl0-0} = 622 nm, λ_{fl0-1} = 671 nm). In contrast, the fluorescence emission spectrum of **10a** (λ_{fl0-0} = 612 nm, λ_{fl0-1} = 658 nm) was blue-shifted. The results are summarized in Table 1 (see Table S1 for *trans*-ABPX

Table 1. Optical Properties of *cis*-ABPX Dyes and RB Dye in Chloroform Containing 2.5% TFA

dye	λ_{abs0-0} [nm]	λ_{fl0-0} [nm]	λ_{abs0-1} [nm]	λ_{fl0-1} [nm]	ε_{0-0} [M^{-1} cm^{-1}]	Φ_{fl}*[a]
ABPX101 **10a**	590	612	545	658	130 300	0.70
ABPX102 **16a**	617	640	567	693	108 200	0.50
ABPX103 **21a**	611	635	562	683	117 000	0.55
ABPX01 **1a**	598	622	553	671	128 650	0.17
RB	552	576	–	–	129 000	0.71

[a]The fluorescence quantum yields of the ABPX dyes were determined by using the reference standard dye RB (ϕ_{fl} = 0.73 in ethanol).

of **10b**, **16b**, and **21b**). **10**, **16**, and **21**, which have almost the same absorption/fluorescence emission maxima in $CHCl_3$, exhibited high ϕ_{fl} values in various solvents (see Figure S3 and Table S2). Both absorption and fluorescence emission spectra were almost unaffected by the change of polarity of the solvents (see Figure S4). Such high quantum yields in various solvents underscore the potential of ABPX dyes for highly sensitive and high-resolution analyses.

A drastic improvement in ϕ_{fl} was achieved by simple modification of ABPX01. However, no marked differences in the molar extinction coefficient (ε) were noted among the ABPX derivatives in Table 1. The rate constant of radiative transition (k_f) is proportional to ε of the ABPX derivatives. The results suggested that the k_f values of the respective ABPX derivatives showed little differences. To further verify the hypotheses that the structurally rigid conjugations around the nitrogen atoms of the xanthene moiety, which enhanced the fluorescence emission efficiency, are related to the reduction of the nonradiative deactivation process, the fluorescence lifetimes (τ_{obs}) of **10a**, **16a**, and **21a** were measured in $CHCl_3$ (containing 2.5% TFA), and k_f and the rate constant of nonradiative transition (k_{nr}) were calculated as shown in Table 2 (see Table S3 for **10b**, **16b**, and **21b**). The fluorescence lifetimes of all the ABPX dyes showed a monoexponential decay (τ_{obs} = 0.72−2.48 ns) in Figures S5−S6. The modified ABPX dyes exhibited longer fluorescence lifetimes than **1**. The k_{nr} values of **10a**, **16a**, and **21a** were much lower than that of **1a** although little difference in k_f was seen among the ABPX derivatives. As we had expected, the enhancement of ϕ_{fl} of **10a**, **16a**, and **21a** was dependent on the marked decrease in k_{nr}.

dx.doi.org/10.1021/ol403262x | *Org. Lett.* 2014, 16, 258−261

Table 2. Fluorescence Quantum Yields, Lifetimes, and Kinetic Constants of *cis*-ABPX Dyes

dye	ϕ_{fl}	τ_{obs} [ns]	k_f [ns^{-1}]	k_{nr} [ns^{-1}]
ABPX01 **1a**	0.17	0.72	0.24	1.06
ABPX101 **10a**	0.70	2.34	0.30	0.30
ABPX102 **16a**	0.50	2.48	0.20	0.32
ABPX103 **21a**	0.55	2.41	0.23	0.32

Whereas the intermolecular rotations of the diethylamino chains of **1a** increased the nonradiative transition probability, reduction of the xanthene moiety mobility was achieved by the inclusion of rigid six-membered rings in $ABPX101H_2^{2+}$–$103H_2^{2+}$, which resulted in the drastic enhancement of ϕ_{fl}. In addition, the ϕ_{fl} of **10a** was higher than that of **16a**. This would be because the torsional motion of the carboxylic benzene moieties was suppressed by the internal steric hindrance caused by the attachment of the carboxylic benzene moieties to the proximate dimethyl of ABPX101. These results showed that RIM played a dominant role in creating the nonradiative deactivation pathways for the decay of the excited states of the ABPX dyes.

In conclusion, we have developed the first highly fluorescent ABPX dyes in the red and NIR regions since the ABPX dye was first reported by our group.[8] The rigid conjugation of the xanthene moiety in the ABPX dyes resulted in high fluorescence quantum yields. ABPX dyes are alternative π-conjugated organic molecules that can be dissolved in commonly used solvents. Our findings demonstrate that ABPX dyes have the potential to act as a substitute for or a complement to existing commercially available fluorescence dyes for use as a new standard for various applications, such as fluorescent probes in molecular imaging, organic electroluminescent devices, and others.

■ ASSOCIATED CONTENT

Supporting Information

Experimental procedures, spectrofluorometric and -photometric spectra, and additional photophysical data for ABPX dyes. This material is available free of charge via the Internet at http://pubs.acs.org.

■ AUTHOR INFORMATION

Corresponding Authors

*E-mail: skamino@riken.jp.
*E-mail: senomoto@pharm.okayama-u.ac.jp.

Notes

The authors declare no competing financial interest.

■ ACKNOWLEDGMENTS

This work was supported by the Adaptable and Seamless Technology Transfer Program through Target-driven R&D (Grant AS242Z01483M) of Japan Science and Technology (JST). This research was also supported in part by a Grant-in-Aid for Challenging Exploratory Research (Grant 24659019) from the Ministry of Education, Culture, Sports, Science and Technology (MEXT) of the Japan Society for the Promotion of Science (JSPS). We thank Dr. Hiroyuki Koshino of RIKEN for NMR measurement and Dr. Yayoi Hongo and Dr. Takemichi Nakamura of RIKEN for MS measurement. We would also like to thank Dr. Toshihiro Shirasaki of Hitachi High-Tech Science Co., Ltd. for support on fluorescence emission analysis. We also thank Ms. Ayako Tohzaka of Okayama University for fruitful discussions.

■ REFERENCES

(1) (a) Yang, Y. J.; Lowry, M.; Xu, X. Y.; Escobedo, J. O.; Sibrian-Vazcluez, M.; Wong, L.; Schowalter, C. M.; Jensen, T. J.; Fronczek, F. R.; Warner, I. M.; Strongin, R. M. *Proc. Natl. Acad. Sci. U.S.A.* **2008**, *105*, 8829. (b) Han, J. Y.; Loudet, A.; Barhoumi, R.; Burghardt, R. C.; Burgess, K. *J. Am. Chem. Soc.* **2009**, *131*, 1642. (c) Anthony, J. E.; Facchetti, A.; Heeney, M.; Marder, S. R.; Zhan, X. W. *Adv. Mater.* **2010**, *22*, 3876. (d) Urano, Y.; Sakabe, M.; Kosaka, N.; Ogawa, M.; Mitsunaga, M.; Asanuma, D.; Kamiya, M.; Young, M. R.; Nagano, T.; Choyke, P. L.; Kobayashi, H. *Sci. Transl. Med.* **2011**, *3*, 110. (e) Wysocki, L. M.; Grimm, J. B.; Tkachuk, A. N.; Brown, T. A.; Betzig, E.; Lavis, L. D. *Angew. Chem., Int. Ed.* **2011**, *50*, 11206. (f) Sibrian-Vazquez, M.; Escobedo, J. O.; Lowry, M.; Fronczek, F. R.; Strongin, R. M. *J. Am. Chem. Soc.* **2012**, *134*, 10502.

(2) (a) Odom, S. A.; Parkin, S. R.; Anthony, J. E. *Org. Lett.* **2003**, *5*, 4245. (b) Mondal, R.; Shah, B. K.; Neckers, D. C. *J. Am. Chem. Soc.* **2006**, *128*, 9612. (c) Anthony, J. E. *Angew. Chem., Int. Ed.* **2008**, *47*, 452.

(3) (a) Yuan, L.; Lin, W. Y.; Zheng, K. B.; He, L. W.; Huang, W. M. *Chem. Soc. Rev.* **2013**, *42*, 622. (b) Kamkaew, A.; Lim, S. H.; Lee, H. B.; Kiew, L. V.; Chung, L. Y.; Burgess, K. *Chem. Soc. Rev.* **2013**, *42*, 77. (c) Nepomnyashchii, A. B.; Bard, A. J. *Acc. Chem. Res.* **2012**, *45*, 1844. (d) Grzybowski, M.; Glodkowska-Mrowka, E.; Stoklosa, T.; Gryko, D. T. *Org. Lett.* **2012**, *14*, 2670. (e) Leblebici, S. Y.; Catane, L.; Barclay, D. E.; Olson, T.; Chen, T. L.; Ma, B. W. *ACS Appl. Mater. Interfaces* **2011**, *3*, 4469. (f) Kolemen, S.; Bozdemir, O. A.; Cakmak, Y.; Barin, G.; Erten-Ela, S.; Marszalek, M.; Yum, J. H.; Zakeeruddin, S. M.; Nazeeruddin, M. K.; Gratzel, M.; Akkaya, E. U. *Chem. Sci.* **2011**, *2*, 949. (g) Umezawa, K.; Nakamura, Y.; Makino, H.; Citterio, D.; Suzuki, K. *J. Am. Chem. Soc.* **2008**, *130*, 1550.

(4) (a) Liu, Y.; Wang, K. R.; Guo, D. S.; Jiang, B. P. *Adv. Funct. Mater.* **2009**, *19*, 2230. (b) Gao, B. X.; Li, H. X.; Liu, H. M.; Zhang, L. C.; Bai, Q. Q.; Ba, X. W. *Chem. Commun.* **2011**, *47*, 3894. (c) Mizoshita, N.; Tani, T.; Inagaki, S. *Adv. Mater.* **2012**, *24*, 3350.

(5) (a) Pron, A.; Gawrys, P.; Zagorska, M.; Djurado, D.; Demadrille, R. *Chem. Soc. Rev.* **2010**, *39*, 2577. (b) Li, L. L.; Diau, E. W. G. *Chem. Soc. Rev.* **2013**, *42*, 291.

(6) Haugland, P. *The Handbook of A Guide to Fluorescent Probes and Labeling Technologies*, 10th ed.; Molecular Probes, Inc.: Eugene, OR, 2005.

(7) Hong, Y. N.; Lam, J. W. Y.; Tang, B. Z. *Chem. Commun.* **2009**, 4332.

(8) Kamino, S.; Horio, Y.; Komeda, S.; Minoura, K.; Ichikawa, H.; Horigome, J.; Tatsumi, A.; Kaji, S.; Yamaguchi, T.; Usami, Y.; Hirota, S.; Enomoto, S.; Fujita, Y. *Chem. Commun.* **2010**, *46*, 9013.

(9) Kamino, S.; Muranaka, A.; Murakami, M.; Tatsumi, A.; Nagaoka, N.; Shirasaki, Y.; Watanabe, K.; Yoshida, K.; Horigome, J.; Komeda, S.; Uchiyama, M.; Enomoto, S. *Phys. Chem. Chem. Phys.* **2013**, *15*, 2131.

(10) Shirasaki, Y.; Kamino, S.; Tanioka, M.; Watanabe, K.; Takeuchi, Y.; Komeda, S.; Enomoto, S. *Chem.—Asian J.* **2013**, *8*, 2609.

(11) Chen, J.; Burghart, A.; Derecskei-Kovacs, A.; Burgess, K. *J. Org. Chem.* **2000**, *65*, 2900.

(12) Sauers, R. R.; Husain, S. N.; Piechowski, A. P.; Bird, G. R. *Dyes Pigment.* **1987**, *7*, 35.